RSC Advances

ROYAL SOCIETY OF CHEMISTRY

www.rsc.org/advances

Graphical abstract

A ternary graphene oxide(GO)/polyacrylamide (PAM)/carboxymethyl cellulose sodium (CMC) nanocomposite hydrogel was fabricated by introducing GO into PAM/CMC hydrogels followed by ionically crosslinking of aluminum ions. The compressive strength of the ternary hydrogel was dramatically enhanced compared with that of the pristine PAM/CMC hydrogels with the incorporation of only 1.6 wt % GO sheets.

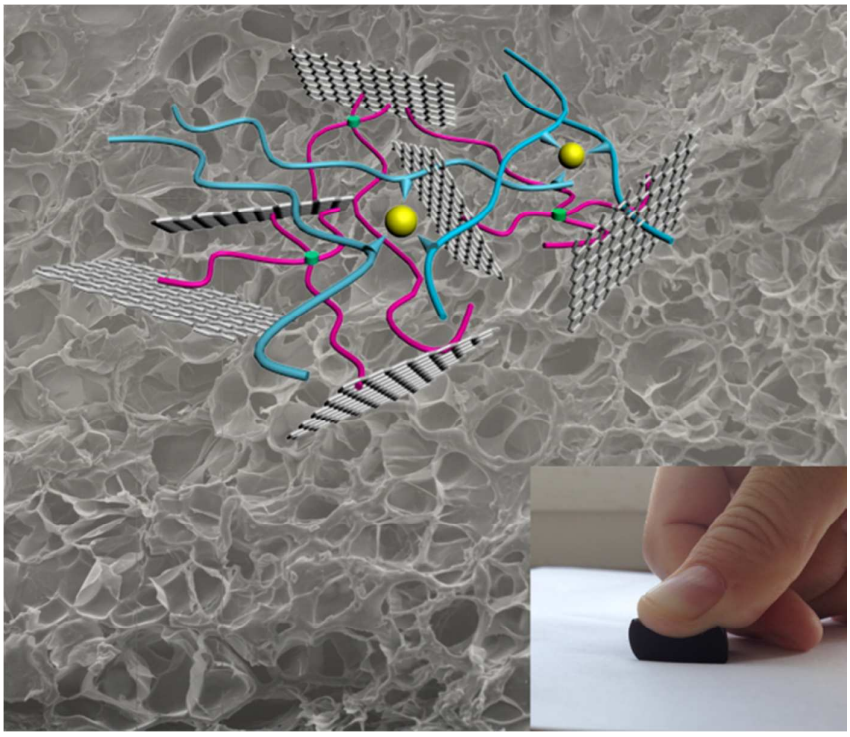

Journal Name

Dynamic Article Links ►

Cite this: DOI: 10.1039/c0xx00000x

www.rsc.org/xxxxxx

ARTICLE TYPE

Graphene oxide/polyacrylamide/carboxymethyl cellulose sodium nanocomposite hydrogel with enhanced mechanical strength: preparation, characterization and the swelling behaviors

Huijuan Zhang,* Dandan Zhai and Yang He

Received (in XXX, XXX) Xth XXXXXXXXX 20XX, Accepted Xth XXXXXXXXX 20XX
DOI: 10.1039/b000000x

A ternary graphene oxide(GO)/polyacrylamide (PAM)/carboxymethyl cellulose sodium (CMC) nanocomposite hydrogel with improved compressive strength was fabricated through free radical polymerization of AM in the presence of GO and CMC in an aqueous system, followed by ionically crosslinking of CMC by aluminium ions. The compressive strength of the ternary hydrogel was dramatically enhanced as compared to that of the pristine PAM/CMC hydrogels with the incorporation of appropriate amount of 1.6 wt % GO sheets. Fourier transform infrared spectroscopy (FT-IR) characterization demonstrated that hydrogen bonding was formed between the oxygen-containing groups of GO sheets with N-H bond of PAM. This strong interaction resulted in the dense structure of the nanocomposite hydrogel and the improved mechanical strength. Moreover, the GO content significantly influenced the swelling behaviors of the composite hydrogels. The kinetic study revealed that the swelling behaviors of nanocomposite hydrogels followed the pseudo-second-order dynamic equation. The strategy of combining GO reinforcement with double network provides an advantageous protocol for the formation of high-strength hydrogel, which may be used in bioengineering and drug delivery system.

1. Introduction

Polymeric hydrogels are typical fascinating and versatile soft materials with wide potential applications in drug delivery and tissue engineering.[1-9] The network structure of hydrogels provides a 3D environment with high water retention, tunable mechanical properties or nutrients. These characters make hydrogels especially appealing for tissue engineering, which seek to restore the function of disease the function of diseased or damaged tissues through the delivery of therapeutic cells with biomaterial scaffolds. [10-12] Generally, the network of the polymeric hydrogels can be formed by covalent cross-linking or non covalent interaction such as hydrogen bonding, van der Waals interactions, or physical entanglements.[13-19] However, most of these hydrogels suffer from poor mechanical performance, which limits their further industrial and biomedical applications. [20, 21] In recent years, much attention has been paid to prepare the hydrogels with superior mechanical properties. [22-28] There are three types of methods to prepare the hydrogels with high strength: a topological (TP) gel, [29] a double network (DN) gel,[30] and a nanocomposite (NC) gel.[31] Among these methods, double network gels and nanocomposite gels are considered to be typical and effective methods to prepare the hydrogels with enhanced mechanical properties. Double network hydrogel refers to a step-wise synthesized hydrogel comprising two independent crosslinked networks. For nanocompsite hydrogels, inorganic fillers such as clays, carbon nanotubes are usually involved in the preparation of the hydrogels as the crosslinkers. [32-34]

Graphene oxide (GO) has stimulated great interest as nanofillers for polymer reinforcement due to its large theoretical special surface area. [35-40] Similar to clays, GO has a layered structure and is rich in oxygen-containing groups, i.e. hydroxyl, epoxide and carboxyl groups. These properties made GO favorable candidates for improving the mechanical strength of the polymeric hydrogels. Yu group incorporated GO into the polyacrylamide (PAM) hydrogels as the crosslinker and demonstrated the reinforcing effect of the GO.[41] Cong et al. prepared GO/poly(acryloyl-6-aminocaproic acid) (PAACA) composite hydrogels with enhanced mechanical properties and self-healing capability. The GO/PAACA composite hydrogel exhibits higher mechanical strength of 65.8 kPa at a stretch of 1190% than that of PAACA hydrogel, with a fracture stress of 8.9 kPa at an elongation of 350%.[42]

* *School of Material and Mechanical Engineering, Beijing Technology Business University, Beijing 100048, China*
†Electronic Supplementary Information (ESI) available: [details of any supplementary information available should be included here]. See DOI: 10.1039/b000000x/

Journal Name

Dynamic Article Links ►

Cite this: DOI: 10.1039/c0xx00000x

www.rsc.org/xxxxxx

ARTICLE TYPE

Carboxymethyl cellulose sodium (CMC) is a representative cellulose derivative, which is a water soluble cellulose ether and manufactured by reacting sodium monochloroacetate with cellulose in alkaline medium.[43-45] So far, many types of CMC-based hydrogels have been developed due to their low toxicity, biocompatibility and economical advantages.[46-48]. Very recently, Yadav et al. prepared a GO/CMC/alginate composite blends by a solution mixing-evaporation method. The incorporation of 1 wt.% GO improved the tensile strength and Young's modulus by 40% and 1128%, respectively. [49] However, it is still a challenge to prepare a mechanically strong hydrogel with GO as a reinforcing filler and CMC as a second network.

As mentioned above, the introduction of a new cross-linked network was considered to be an effective way to prepare the hydrogels with enhanced mechanical strength. CMC is a polymer with multiple carboxyl groups, exhibits excellent coordination abilities with metal ions. It can form hydrogels in the presence of metal ions (such as Al^{3+}) via the coordination between metal ions and the carboxyl groups in the polymer side chains. Considering the good coordination ability and biodegradability of CMC, it is a good choice to prepare DN hydrogels with CMC as the second network which could be cross-linked by simple coordination with metal ions.

In the present work, we successfully prepared a new kind of nanocomposite hydrogel by introducing GO into the PAM/CMC hydrogels followed by ionically crosslinking of aluminum ions. The schematic diagram of GO/PAM/CMC ternary nanocomposite hydrogel was illustrated in Scheme. 1. The layered GO nanosheets were intercalated with the polymer networks of hydrogel. The load transfer between the polymer chains of hydrogel and GO nanosheets is beneficial for mechanical improvement of the hydrogel due to the large surface area of the GO nanosheets. There are two types of crosslinked polymer: ionically (Al^{3+}) crosslinked CMC and covalently crosslinked PAM in the network structure of the PAM/CMC hydrogel. When the GO nanosheets were introduced into the PAM/CMC hydrogel, the new chemical crosslinking points comes from GO nanosheets were produced in the structure of GO/PAM/CMC hydrogel. Additionally, the functional groups of GO nanosheets also offer hydrogen bonding with polymer chains. As a result, the GO nanosheets can act as reinforcing nanofillers for further enhancing the mechanical performance of the PAM/CMC hydrogel. This GO/PAM/CMC hydrogels exhibited superior mechanical properties compared with the reported GO composite hydrogels and aluminum ions composite hydrogels. Additionally, CMC was applied in our work, which is biocompatible and made this hydrogel suitable in the bio-related areas. This strategy of the combination of the double network and GO reinforcement to prepare high-strength hydrogel was simple and practicable.

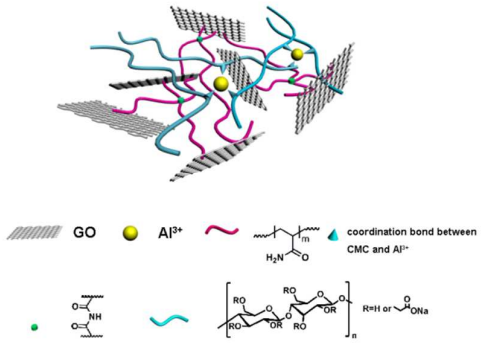

Scheme 1 Schematic diagram of GO/PAM/CMC ternary nanocomposite hydrogel.

The microstructure and properties of the hydrogels were characterized with scanning electron microscopy (SEM), Fourier transform infrared (FT-IR) spectroscopy, X-ray diffraction (XRD) and thermogravimetric (TG). Compressive tests of the composite hydrogel were used to study its mechanical properites. To further reveal the structural features of the composite hydrogels, swelling behaviors of the pristine PAM/CMC and GO/PAM/CMC hydrogels were systematically investigated. Considering that the release of aluminum ions can decrease biocompatibility,[50] it might be unsuitable for the specific system for in vitro use. Substituting Mg^{2+} ions for Al^{3+} ions may be more favorable due to its better biocompatibility.

2 Experimental

2.1. Materials

Journal Name

Dynamic Article Links ►

Cite this: DOI: 10.1039/c0xx00000x

www.rsc.org/xxxxxx

ARTICLE TYPE

Graphene oxide was obtained from Nanjing XFNANO Materials Tech Co., Ltd. Carboxymethyl cellulose sodium (CMC) (800~1200 mPa.s CP), acrylamide (AM), ammonium persulfate (APS), N, N'-methylenebisacrylamide (MBA), aluminum nitrate hydrate ($Al(NO_3)_3 \cdot 9H_2O$) were purchased from Sinopharm Chemical Reagent Co. Ltd (SCRC) and used without further purification.

2.2 Preparation of the ternary composite hydrogels

Hydrogels were prepared by a simple mixture and solution polymerization using initial solutions consisting of monomers (GO, CMC and AM), crosslinker (MBA), initiator (APS). Typical procedure was as follows: Firstly, the desired amount of dried GO was exfoliated and dispersed in 10 mL of water by sonication. Successively, 0.10 g CMC was added and dissolved in the above GO aqueous dispersion under magnetic stirring and sonication at room temperature until the solution became uniform. Then 2.4 g AM, 0.024 g APS and 0.036 g MBA were added and stirred at 0 °C, and then 0.02 g of APS and 0.03 g MBA was added. After magnetic stirring for 2 h at 0 °C, the homogeneous mixture solutions were transferred into a glass tube and kept for hydrogel formation at 80 °C for 2 h. Herein, APS was used as a peroxide initiator, which was sensitive to the temperature and may be initiated before the mixed solution became homogeneous, which may lead to the imperfection of the hydrogels. In order to prevent possible polymerization during the stirring process, lower temperature, i.e. 0 °C was applied while stirring. After the hydrogel formation, the ternary composite hydrogels, in their cylindrical form, were taken out of the glass tube and put into de-ionized (DI) water to remove homopolymers and unreacted monomers. Then the hydrogels were immersed into the 4 wt% $Al(NO_3)_3$ aqueous solution with Al^{3+} ionically crosslinking for 24 h. Finally, the hydrogels were placed into DI water for 1 week (Table 1). In this paper, hydrogels are expressed as GO_m/PAM/CMC hydrogels, where m represents the weight percent of GO sheets relative to the total amount of AM and CMC.

Table 1 The feed compositions of the hydrogels.

Sample	AM (g)	CMC (g)	APS (g)	MBA (g)	GO (g)	H_2O (mL)
PAM/CMC	2.4	0.10	0.024	0.036	-	10
$GO_{0.8}$/PAM	2.4	-	0.024	0.036	0.020	10
$GO_{0.4}$/PAM/CMC	2.4	0.10	0.024	0.036	0.010	10
$GO_{0.8}$/PAM/CMC	2.4	0.10	0.024	0.036	0.020	10
$GO_{1.2}$/PAM/CMC	2.4	0.10	0.024	0.036	0.030	10
$GO_{1.6}$/PAM/CMC	2.4	0.10	0.024	0.036	0.040	10

2.3 Characterization

Fourier transform infrared spectroscopy (FT-IR) spectra were recorded on an iN10MX spectrometer. X-ray powder diffraction (XRD) patterns were recorded on an Empyrean XRD with Cu-Kα radiation (λ=1.54056 Å) over a 2θ range of 5–90°. Thermogravimetric analyses (TGA) were conducted with Q5000IR, heating samples from ambient temperature to 700 °C at the heating rate of 20 °C min^{-1} in a nitrogen atmosphere. The internal network structures of hydrogels were characterized by scanning electron microscopy (SEM) (QUANTA FEG 250). Prior to conduct SEM characterization, the hydrogels are firstly freeze-dried to obtain the dried samples. Then the freeze-drying samples are cut into slices by a knife and sprayed by gold to give good electrical conductivity. To obtain a clear observation of the inner structure of the hydrogels, the sample table was rotated so that the lens was perpendicular to the pores of the samples. Rheological properties of $GO_{0.4}$/PAM/CMC, $GO_{0.8}$/PAM/CMC $GO_{1.6}$/PAM/CMC hydrogels were conducted with HAAKE MARS III rheometer using parallel plates of diameter 20 mm at 25 °C. The gap between the two parallel plates was set at 1 mm. The frequency sweep was performed over the frequency range of 0.01-10 rad/s.

2.4 Equilibrium swelling degree of hydrogel

The dried hydrogels were immersed in distilled water until their weight became constant. The hydrogles were then removed from the water and their surfaces were blotted with filter paper before weighed. The swelling ratio was calculated with the following equation.

$$\text{Swelling ratio} = \frac{W_s - W_d}{W_d}$$

Journal Name

Dynamic Article Links ►

Cite this: DOI: 10.1039/c0xx00000x

www.rsc.org/xxxxxx

ARTICLE TYPE

(1)

where W_d and W_s represent the weights of the dried hydrogel and the hydrogel at swelling equilibrium state, respectively.

2.5 Compressive tests of hydrogels

The mechanical properties of the hydrogels were tested using a CMT6104 universal testing machine. For the compressive tests, the hydrogel samples (column, with a diameter of 18 mm and height of 15 mm) were placed between the self-leveling plates. The samples were compressed at a rate of 20 mm min^{-1} until the compression ratio reached 80%.

3 Results and discussion

3.1 Preparation and characterization of the hydrogels

In a typical synthesis, GO was firstly exfoliated and dispersed in deionized water under ultrasonication. Then CMC, AM, initiator and crosslinker were added to the GO dispersion. Subsequently, the GO/PAM/CMC ternary composite hydrogel was fabricated by initiating the polymerization of AM attached to the GO nanosheets with the help of ammonium persulfate as an initiator and BIS as a crosslinker. The obtained hydrogel was then immersed into the $Al(NO_3)_3$ aqueous solution to coordinate with the carboxyl groups in CMC and form another interconnected network. GO nanosheets had the advantages of being easily functionalized and high dispersibility in aqueous medium due to the abundant carboxyl groups at the GO edges and epoxy and hydroxy groups on the planes. On the one hand, GO nanosheets interact with the PAM network by hydrogen bonding to form an interwined network. On the other hand, CMC formed another interconnected network originating from the coordination interactions between carboxyl groups and Al^{3+}.

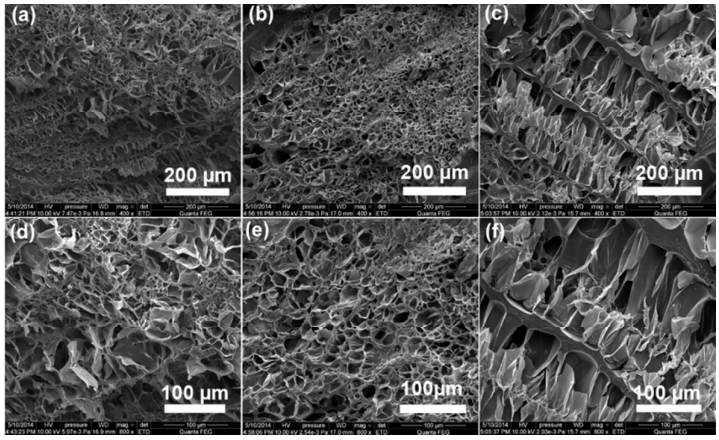

Fig. 1 SEM images of the lyophilized hydrogels. (a) $GO_{0.4}$/PAM/CMC, (b) $GO_{1.6}$/PAM/CMC, (c) PAM/CMC, (d) a local partial enlarged image of (a), (e) a local partial enlarged image of (b), (f) a local partial enlarged image of (c).

SEM was used to characterize and explore the variation trend of the inner structures of the hydrogels with the incorporation of GO. PAM/CMC, $GO_{0.4}$/PAM/CMC and $GO_{1.6}$/PAM/CMC hydrogels were used as typical samples to characterize the internal microstructures, which represent the pristine hydrogels and those with the lowest and the highest amount of GO. The typical SEM images of the lyophilized hydrogels were depicted in Fig 1. For $GO_{0.4}$/PAM/CMC hydrogel (Fig. 1(a) and (d)), the morphology is characterized by filamentous structures with interconnecting pores inside and outside the holes of the hydrogel. The hydrogel shows a 3D network structure with no obvious aggregation of GO nanosheets. It is interesting to note that the pore size of the hydrogel becomes smaller when the amounts of GO increased ($GO_{1.6}$/PAM/CMC), implying a denser structure of the hydrogel (Fig. 1(b) and (e)). This can be attributed to the stronger hydrogen-bonding interaction between oxygen-containing groups of GO and polar functional groups of the PAM side chains. Oppositely, as shown from Fig 1 (c) and (f), the PAM/CMC hydrogel prepared under identical conditions as the ternary composite hydrogel in the absence of GO, exhibited a thick block with sparse pores dispersed.

Journal Name

Dynamic Article Links ►

Cite this: DOI: 10.1039/c0xx00000x

www.rsc.org/xxxxxx

ARTICLE TYPE

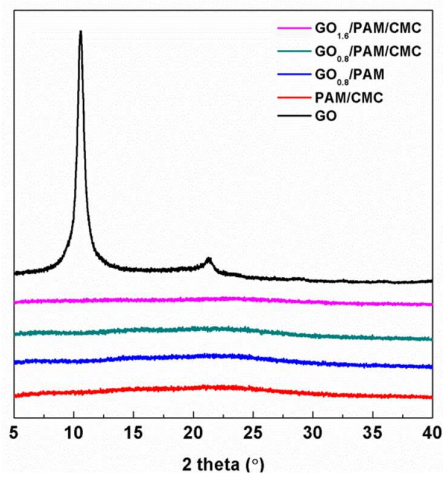

Fig. 2 XRD patterns of GO sheets, PAM/CMC, $GO_{0.8}$/PAM, $GO_{0.8}$/PAM/CMC and $GO_{1.6}$/PAM/CMC hydrogels.

Fig. 2 shows the XRD patterns of GO, PAM/CMC, $GO_{0.8}$/PAM and $GO_{0.8}$/PAM/CMC hydrogels. The diffraction pattern of pure GO has a peak at 2θ=10.6°, corresponding to the interplanar distance between GO sheets.[51] There was no characteristic GO peak at 10.6° detected in the XRD pattern of PAM/CMC, $GO_{0.8}$/PAM, $GO_{0.8}$/PAM/CMC hydrogels and $GO_{1.6}$/PAM/CMC hydrogels, suggesting that GO nanosheets were uniformly dispersed in the polymer gels without ordered aggregation.

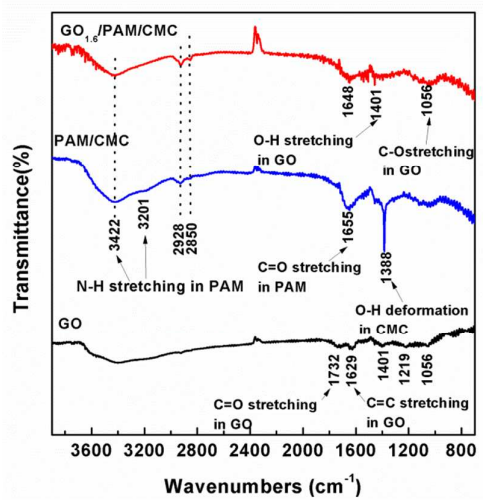

Fig. 3 FT-IR spectra of GO powder, PAM/CMC hydrogel and $GO_{1.6}$/PAM/CMC hydrogel.

Possible interactions between GO nanosheets and polymer chains were clarified by analyzing the FT-IR spectra of GO powder, PAM/CMC hydrogel, and GO1.6/PAM/CMC hydrogel (Fig. 3). GO and PAM/CMC were used as comparison of $GO_{1.6}$/PAM/CMC to explore the differences between the FI-IR spectra before and after the incorporation of GO powder. $GO_{1.6}$/PAM/CMC hydrogel sample, with the highest amount of GO powder, exhibited the most distinct peaks in the spectrum. The obvious peaks at 1732, 1629, 1401, 1219, and 1056 cm^{-1} in the FT-IR spectrum of GO powder were attributed to C=O carbonyl stretching, aromatic C=C stretching, O−H deformation vibration, and asymmetric and symmetric C−O stretching in C−O−C group, respectively .[52]

In the FT-IR spectrum of PAM/CMC hydrogel, the bands at 3422, 3201, 2928, and 2850 cm^{-1} in the high-frequency region were characteristic of N−H stretching and asymmetric and symmetric vibration of C−H

Journal Name

Dynamic Article Links ►

Cite this: DOI: 10.1039/c0xx00000x

www.rsc.org/xxxxxx

ARTICLE TYPE

stretching, respectively.[43] The peak at 1655 cm^{-1} can be ascribed to the characteristic C=O stretching of PAM. Another strong band at 1388 cm^{-1} was related to O−H deformation of the carboxylic acid group in CMC.

In the FT-IR spectrum of $GO_{1.6}$/PAM/CMC hydrogel, most of the bands belonging to GO powder were significantly decreased (1401 and 1056 cm^{-1}) or even disappeared (1732, 1629 and 1229 cm^{-1}). Furthermore, the C=O stretching (1655 cm^{-1}) in the PAM/CMC hydrogel shifted to the lower wavenumber of 1648 cm^{-1}. And the marked typical O−H deformation at 1388 cm^{-1} and N-H stretching of PAM at 3201 cm^{-1} disappeared. The disappearance of the featured bands suggested intertwined networks in the $GO_{1.6}$/PAM/CMC hydrogel through hydrogen bonding of oxygen-containing groups of GO sheets with N-H bond of PAM. [53, 54]

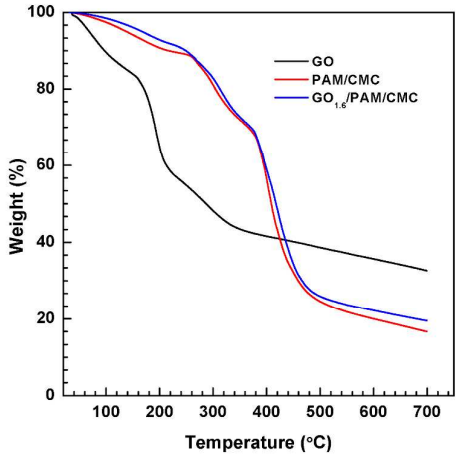

Fig. 4 TGA curves of GO sheets, PAM/CMC and $GO_{1.6}$/PAM/CMC hydrogels.

TGA curves of the GO sheets, PAM/CMC and $GO_{1.6}$/PAM/CMC hydrogels were shown in Fig. 4, which was used to indicate the changes of thermal stability of the hydrogels before and after the addition of GO powder. As shown in Fig. 4, GO was thermally unstable and more than 40% of its weight loss took place even below 200 °C, which was assigned to the decomposition of the labile oxygen containing functional groups. [51, 55] It can also be observed that the incorporation of GO increased the thermal stability of the PAM/CMC hydrogels, suggesting a strong interaction between the GO sheets and polymer chains. Additionally, GO content in $GO_{1.6}$/PAM/CMC hydrogels can be estimated to be 1.64 wt% according to TGA measurements, which is very close to the original feed ratio. It reveals that the GO sheets participate in the cross-linking reaction efficiently in the water.

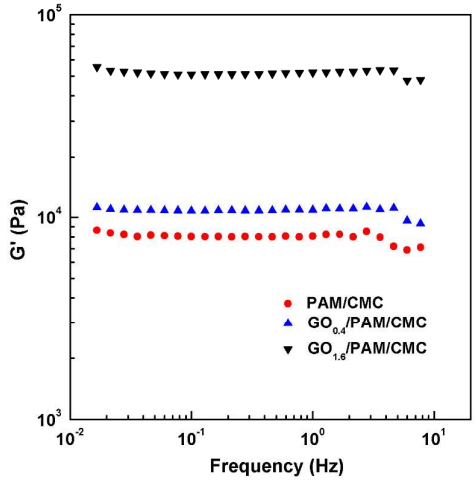

Fig. 5 Dependence of storage modulus (G') at 25°C for PAM/CMC, $GO_{0.4}$/PAM/CMC, $GO_{1.6}$/PAM/CMC hydrogels.

Journal Name

Dynamic Article Links ►

Cite this: DOI: 10.1039/c0xx00000x

www.rsc.org/xxxxxx

ARTICLE TYPE

To investigate the rheological behaviors of the hydrogels, the dynamic viscoelastic properties were examined by a rheometer. Fig. 5 shows the storage modulus (G') of the PAM/CMC, $GO_{0.4}$/PAM/CMC, $GO_{1.6}$/PAM/CMC hydrogels as a function of the frequency. The oscillatory tests were conducted in the frequency range of 0.01-10 $rad.s^{-1}$. As shown in Fig. 5, the three hydrogel samples show the typical gel rheological behaviors. The G' of the three hydrogel samples shows little change in the tested frequency range, which is characteristic of gels with a high degree of crosslinking. The small variation when the frequency was greater than 50 Hz is negligible, which may be caused by the preparation of the sample when performing the tests. The similar phenomenon can also be seen in the study by Chen et al. [56] The frequency sweeping results also demonstrate the reinforcing effect of GO sheets, and more GO sheets lead to a stronger hydrogel. This is mainly because the strong interaction between GO and polymer chains provides high crosslinking strength.[39]

3.2 Mechanical properties of the hydrogels

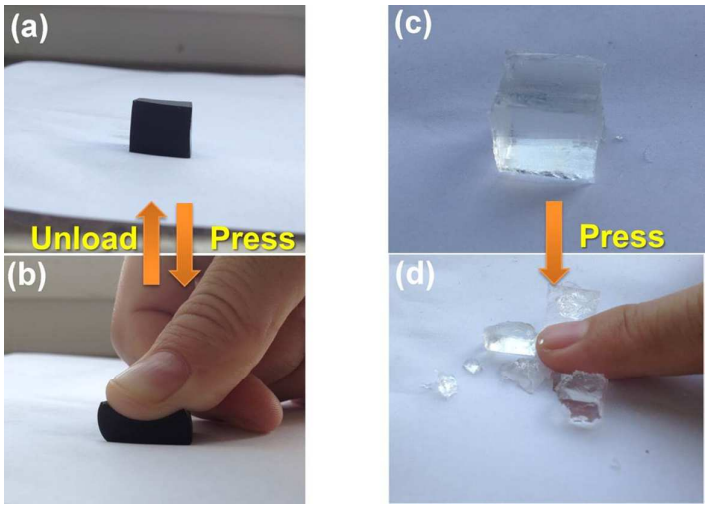

Fig. 6 Photographs of $GO_{1.6}$/PAM/CMC and PAM/CMC hydrogels under pressure.

The obtained $GO_{1.6}$/PAM/CMC hydrogel displayed high performance in compressive strength and ductility. The $GO_{1.6}$/PAM/CMC hydrogel is tough enough to withstand high deformations in compression without obvious damage. As shown in Fig. 6a and b, $GO_{1.6}$/PAM/CMC hydrogel was not damaged after compression under pressure. Upon removing of the compression force, the $GO_{1.6}$/PAM/CMC hydrogel quickly recovers its original shape. In contrast, the counterpart without the introduction of GO was broken on compression due to its brittleness, as shown in Fig. 6c and d.

Compressive tests were used to characterize the mechanical properties of the hydrogels. The pristine PAM/CMC hydrogel is very brittle, so the compressive tests were not performed. The compressive tests were conducted on the $GO_{0.8}$/PAM hydrogel to determine the influence of the second layer of network on the mechanical properties of the ternary composite hydrogels. As shown in Fig. 7, the compressive strength of the $GO_{0.8}$/PAM hydrogel is ~0.759 MPa at the compressive deformation of ~60%. For $GO_{0.8}$/PAM/CMC hydrogel, the compressive strength is 1.04 MPa, increased by ~37% compared with with the $GO_{0.8}$/PAM hydrogel. Considering the same GO and AM contents except for the presence of CMC network in these two samples, it is thus proposed that the introduction of the second CMC network was favorable for improving the compressive strength of the ternary composite hydrogel. It can also be observed that the increase in the amount of GO resulted in the dramatic enhancement of the compressive strength of the ternary composite hydrogel. The compressive strength of the $GO_{1.6}$/PAM/CMC hydrogel reached 2.87 MPa, increased by ~260% compared with the $GO_{0.4}$/PAM/CMC hydrogel.

Journal Name

Dynamic Article Links ►

Cite this: DOI: 10.1039/c0xx00000x

www.rsc.org/xxxxxx

ARTICLE TYPE

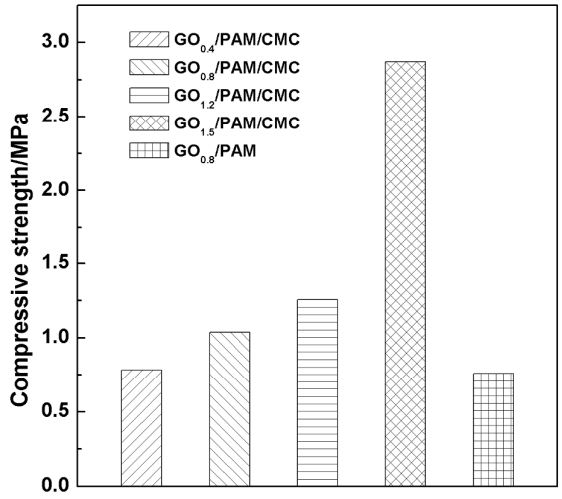

Fig. 7 Compressive strength of $GO_{0.8}$/PAM and GO/PAM/CMC hydrogels with different amounts of GO.

Evidently, the incorporation of GO can improve the mechanical properties of PAM/CMC hydrogels. For GO/PAM binary nanocomposite hydrogels, GO participated in radical chain transfer reactions during the free radical polymerization, leading to the grafting of PAM macromolecules onto the layered GO sheets. As a result, the GO nanosheets acted as fresh chemical crosslinking points in hydrogel formation.[41, 53] For GO/PAM/CMC ternary nanocomposite hydrogels, the compressive strength is higher as shown in Fig. 7. It is mainly attributed to the synergy of GO reinforcement and the formation of the double network. Taken together, the introduction of GO into the PAM/CMC DN hydrogels further improved their mechanical properties.

3.3 Swelling behaviors of the hydrogels

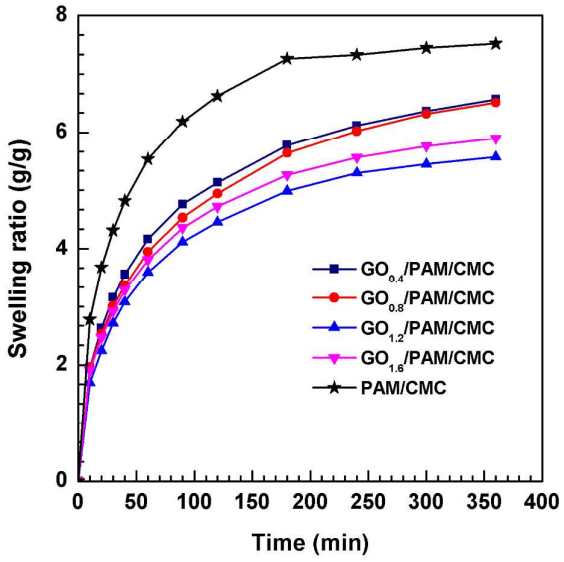

Fig. 8 Swelling rates of PAM/CMC and GO/PAM/CMC hydrogels in deionized water.

The swelling behavior was systematically investigated to further reveal the structural features of the composite

Journal Name

Dynamic Article Links ►

Cite this: DOI: 10.1039/c0xx00000x

www.rsc.org/xxxxxx

ARTICLE TYPE

hydrogels. It is well known that the swelling behavior of the hydrogel depended on the crosslinked density of the gel network.[57, 58] As shown in Fig. 8, the swelling rates of both pure and composite hydrogels were quick at the initial stage and then began to level off. The swelling equilibrium could be achieved within about 200 min. It can also be observed that the PAM/CMC hydrogel presented a faster rate of absorbing water and higher swelling ratio than the GO/PAM/CMC hydrogels, which is consistent with the results of other researchers.[41, 42] Herein, the GO nanosheet was regarded as a kind of cross-linker and formed more cross-link points with higher cross-linked density, resulting in reduction of swelling capacities. The differences in swelling behaviors confirmed the more robust network of the GO/PAM/CMC hydrogel than that of the PAM/CMC hydrogel.

Meanwhile, the swelling ratio of the GO/PAM/CMC hydrogels decreased with the increasing GO loadings to 1.2 wt.% and then slightly increased with the further increase of GO loadings. The reason may be as follows: There are two competing effects in the GO/PAM/CMC nanocomposite hydrogels in terms of swelling capacity. On the one hand, the incorporation of the GO sheets tends to interact with PAM chains and increase the cross-linked density, which would result in the decreased swelling ratio.[42] On the other hand, the GO sheets contain plenty of functional groups on the surface, which would increase the density of hydrophilic groups on the polymer networks and exert a positive effect in the swelling capacity.[53] In the $GO_{1.2}$/PAM/CMC and $GO_{1.6}$/PAM/CMC hydrogels, the amount of the functional groups of the PAM and CMC was the same, with the premise that the AM monomer reacted completely during polymerization. The ratio of functional groups of GO of the two samples is 1: 1.5. Thus, the ratio of the functional groups of GO: PAM: CMC of the two samples is 1.5: 1. The increased GO in $GO_{1.6}$/PAM/CMC contained more hydrophilic functional groups and resulted in the higher swelling ratio than $GO_{1.2}$/PAM/CMC hydrogel. However, this effect was moderate and the swelling ratio of the $GO_{1.6}$/PAM/CMC hydrogel was still lower than that of the $GO_{0.8}$/PAM/CMC hydrogel and $GO_{0.4}$/PAM/CMC. The similar swelling behaviors of $GO_{0.4}$/PAM/CMC and $GO_{0.8}$/PAM/CMC hydrogels may be the combination of the above effects.

Table 2. Results obtained from linear regression of the different kinetics equations.

GO content (%)	Fickian model			Schott model			
	n	K ($g \cdot g^{-1} \cdot min^{-0.3}$)	R^2	$K \times 10^{-3}$ ($min^{-1} \cdot g \cdot g^{-1}$)	W_e (fitting data, g/g)	W_e (experimental data, g/g)	R^2
0	0.2917	0.2080	0.9988	5.066	8.053	7.518	0.9994
0.4	0.3472	0.1443	0.99965	3.572	7.159	6.563	0.9972
0.8	0.3489	0.1399	0.9981	3.257	7.152	6.511	0.9951
1.2	0.3471	0.1467	0.9921	4.353	6.100	5.569	0.9980
1.6	0.3296	0.1598	0.9959	4.308	6.412	5.893	0.9976

There are many influence factors affecting the water diffusion mode of the gel and the rate of water diffusion. The influence factors include stress relaxation of polymers,[59] crosslink concentration [60] and ionic groups on polymer networks.[61, 62] To further explore the mechanisms of water diffusion of the hydrogels, kinetic model studies were performed. It is well-known that the initial water uptake process of hydrogels corresponds to the diffusion of water molecules into the gel network. To investigate the diffusion model of the hydrogels, the initial swelling data were fitted to the exponential heuristic equation for $W/W_e \leq 0.5$

$$W/W_e = Kt^n \quad (2)$$

where W was the swelling ratio of the hydrogel at time t, W_e was the swelling ratio of the hydrogel at equilibrium, K was the rate constant and n is a characteristic exponent. The plot of $\lg(W/W_e)$ against $\lg t$ is shown in Fig. 9. It is clear that the linear relations are obtained. The values of n and K can be calculated from the slope and intercepts of the lines as shown in Table 2.

Journal Name

Dynamic Article Links ►

Cite this: DOI: 10.1039/c0xx00000x

www.rsc.org/xxxxxx

ARTICLE TYPE

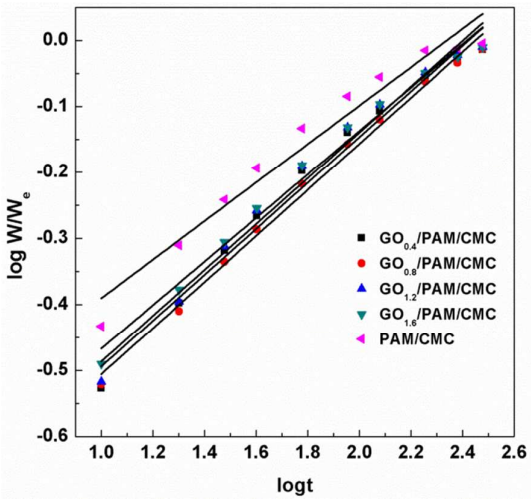

Fig. 9 Plots of log(W/W_e) against log t for the nanocomposite hydrogels.

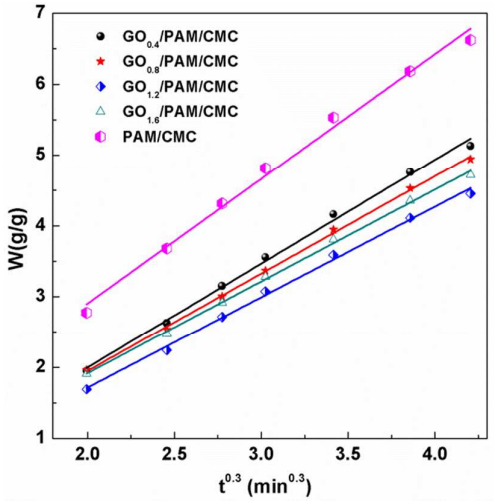

Fig. 10 W-$t^{0.3}$relation curve of PAM/CMC and GO/PAM/CMC hydrogels in the time range of 10 and 120 min in deionized water.

It can be found that the value of n for the composite hydrogels are ~0.3 regardless of the amount of GO. The result indicates that the diffusion rate for water penetrated into the composite hydrogels is low and the transport process is diffusion-controlled. (Fickian diffusion) The swelling kinetics of the PAM/CMC and GO/PAM/CMC composite hydrogels in deionized water was discussed by a Fickian and a Schott model, respectively[47, 63-64] Unfortunately, the entire swelling process did not exhibit Fickian behavior. The main reason is that for an extensive swelling system the diffusion coefficient obviously did not remain constant, which is the premise of Fickian law. Therefore, the swelling kinetics of the PAM/CMC and GO/PAM/CMC composite hydrogels was discussed by Fickian model in the time range of 10 and 120 min, as shown in Fig. 10. Clearly, the plot of W vs. $t^{0.3}$ showed a linear relationship, which indicates that the initial swelling process exhibits Fickian behavior. Correspondingly, the values of R^2 were higher than 0.99 (Table 2). It is assumed that the extensive swelling processes follow the Schott second order kinetics. For Schott model, the swelling rate the swelling rate at any time was expressed as follows:

Journal Name

Dynamic Article Links ►

Cite this: DOI: 10.1039/c0xx00000x

www.rsc.org/xxxxxx

ARTICLE TYPE

$$\frac{dW}{dt} = K(W_e - W)^2 \quad (2)$$

where W was the swelling ratio of the hydrogel at time t, W_e was the swelling ratio of the hydrogel at equilibrium and K was the rate constant. The integration form in scope [0, t] and [0, W_t] can be represented as follows:

$$\frac{1}{W_e - W} = Kt + \frac{t}{W_e} \quad (3)$$

And then Eq. (3) could be reorganized to obtain a linear form:

$$\frac{t}{W} = \frac{1}{K \cdot W_e^2} + \frac{t}{W_e} \quad (4)$$

By plotting a graph of t/W versus t, a straight line with a slope of $1/W_e$ and an intercept of $1/(K \cdot W_e^2)$ could be obtained. From this plot, the swelling capacity (W_e) and the swelling rate constant (K) could be evaluated by the slope and intercept. The results are summarized and presented in Table 2. It can be observed from Fig. 11 that the plot of t/W versus t showed a linear relationship and the values of R^2 of all the hydrogels are higher than 0.99 (Table 2), suggesting that the experimental data were well fitted by the Schott model. From Table 2, the theoretical analyses data of W_e were well consisted with the experimental data for all the hydrogels. Therefore, it is suitable to apply the Schott model to discuss the swelling kinetics of the GO/PAM/CMC nanocomposite hydrogels. Additionally, the PAM/CMC hydrogel exhibited the highest theoretical and experimental swelling capacity and the swelling rate constant (K). This may be ascribed to the loose inner structure of PAM/CMC hydrogels and the larger pores in the network (shown in Fig. 1), which is favorable for the diffusion of water molecules.

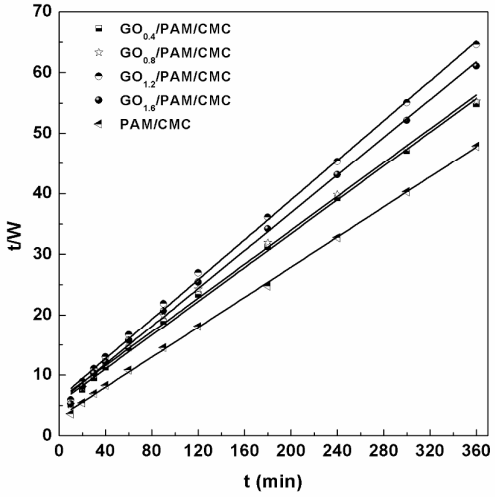

Fig. 11 *t/W-t* relation curve of PAM/CMC and GO/PAM/CMC hydrogels in deionized water.

Conclusions

In summary, a novel ternary GO/PAM/CMC nanocomposite hydrogel system with improved mechanical strength has been designed and synthesized by the strategy of the combination of double network and nanofiller reinforcement. The compressive strength of the ternary $GO_{1.6}$/PAM/CMC nanocomposite hydrogel achieved 2.87 MPa, which can be ascribed to the hydrogen bonding between GO and polymer chains demonstrated by the FT-IR results. The second network formed by Al^{3+} ionically crosslinking of CMC also contributed to improving the

Journal Name

Dynamic Article Links ►

Cite this: DOI: 10.1039/c0xx00000x

www.rsc.org/xxxxxx

ARTICLE TYPE

compressive strength, indicating the importance of the cross-linking density. Moreover, the swelling behaviors of the composite hydrogels were greatly related to the content of GO and the swelling processes of nanocomposite hydrogels followed the pseudo-second-order dynamic equation. This strategy provides an advantageous protocol for the formation of high-strength hydrogel, especially the CMC-based hydrogels. Considering its high strength and the favorable biocompatibility, it is anticipated that this hydrogel may be used in bioengineering and drug delivery system.

Acknowledgements

We acknowledge supports from National Nature Science Foundation of China (NO. 21104040) and China Postdoctoral Science Foundation (NO. 2013M540927).

Notes and references

1 D. J. Pochan, J. P. Schneider, J. Kretsinger, B. Ozbas, K. Rajagopal and L. Haines, *J. Am. Chem. Soc*., 2003, **125**, 11802-11803.
2 G. Chen and A. S. Hoffman, *Nature*, 1995, **273**, 49-52.
3 S. Keun, K. Sung, W. Young, H. Jin, Y. Ji and H. Soon, *Biomaterials*, 2004, **25**, 2393-2398.
4 A. Gutowska, Y. H. Bae, H. Jacobs, J. Feijen and S. W. Kim, *Macromolecules*, 1994, **27**, 4167-4175.
5 F. llman, T. Tanaka and E. Kokufuta, *Nature*, 1991, **349**, 400-401.
6 C. Tsitsilianis, *Soft Matter*, 2010, **6**, 2372-2388.
7 Z. Yang, S. Pickard, N. J. Deng, R. J. Barlow, D. Attwood, C. Booth, *Macromolecules*, 1994, **27**, 2371-2379.
8 G. T. Gotzamanis, C. Tsitsilianis, S. C. Hadijyannakou, C. S. Patrickios, R. Lupytsky and S. Minko, *Macromolecules*, 2006, **39**, 678-683.
9 Z. S. Ge, J. M. Hu, F. H. Huang and S. Y. Liu, *Angew. Chem. Int. Ed.*, 2009, **48**, 1798-1802.
10 F. Zhao , M. Ma and B. Xu , *Chem. Soc. Rev.,* 2009 , **38** , 883-891.
11 K. Y. Lee and D. J. Mooney , *Chem. Rev.,* 2001 , **101** , 1869-1879 .
12 B. V. Slaughter , S. S. Khurshid , O. Z. Fisher , A. Khademhosseini and N. A. Peppas , *Adv. Mater.*, 2009 , **21** , 3307 -3329.
13 P. D. Topham, J. R. House, O. O. Mykhaylyk, S. P. Armes, R. A. L Jones and A. J. Ryan. *Macromolecules*, 2006, **39**, 5573-5576.
14 N. Stavrouli, T. Aubry and C. Tsitsilianis, **Polymer**, 2008, **49**, 1249-1256.
15 M. Lemmers, J. Sprakel, I. K. Voets, J. Gucht and M. A. C. Stuart, *Angew. Chem. Int. Ed.*, 2010, **49**, 708-711.
16 W. Z. Yuan, X. F. Li, S. Y. Gu, A. M. Cao and J. Ren, *Polymer*, 2011, **52**, 658-666.
17 C. Li, J. Madsen, S. P. Armes and A. L. Lewis, *Angew. Chem. Int. Ed.*, 2006, **45**, 3510-3513.
18 L. Ma, H. L. Kang, R. G. Liu and Y. Huang , *Langmuir*, 2010, **26**, 18519-18525.
19 L. Ma, R. G. Liu, J. J. Tan, D. Q. Wang, X. Jin, H. L. Kang, M. Wu and Y. Huang, *Langmuir*, 2010, **26**, 8697-8703.
20 H. Itagaki, T. Kurokawa, H. Furukawa, T. Nakajima, Y. Katsumoto and J P. Gong, *Macromolecules*, 2010, **43**, 9495-9500.
21 T. Nakajima, H. Furukawa, Y. Tanaka, T. Kurokawa, Y. Osada and J. P. Gong, *Macromolecules*, 2009, **42**, 2184-2189.
22 J. P. Gong, Y. Katsuyama, T. Kurokawa and Y. Osada, *Adv. Mater*., 2003, **15**, 1155-1158
23 K. Yasuda, J. P. Gong, Y. Katsuyama, A. Nakayama, Y. Tanabe, E. Kondo, M. Ueno and Y. Osada, *Biomater*. 2005, **26**, 4468-4475.
24 Y. H. Na, T. Kurokawa, Y. Katsuyama, H. Tsukeshiba., J. P. Gong, Y. Osada, S. Okabe, T. Karino and M. Shibayama, *Macromolecules*, 2004, **37**, 5370-5374.
25 Y. Tanaka, R. Kuwabara, Y. H. Na, T. Kurokawa, J. P. Gong and Y. Osada, *J. Phys. Chem. B*, 2005, **109**, 11559-11562
26 H. Tsukeshiba, M. Huang, Y. H. Na, T. Kurokawa, R. Kuwabara, Y. Tanaka, H. Furukawa, Y. Osada and J. P. Gong, *J. Phys. Chem. B*, 2005, **109**, 16304-16309
27 T. Kurokawa, H. Furukawa, W. Wang, Y. Tanaka and J. P. Gong, *Acta Biomaterialia*, 2010, **6**, 1353-1359.
28 J. J. Saito, H. Furukawa, T. Kurokaw, R. Kuwabara, S. Kuroda, J. Hu, Y. Tanaka, J. P. Gong, N. Kitamurae and K. Yasudae, *Polym. Chem.* 2011, **2**, 575-580.
29 Y. Okumura and K. Ito, *Adv. Mater.*, 2001, **13**, 485-487.
30 J. P. Gong, *Soft Matter*, 2010, **6**, 2583-2390.
31 K. Haraguchi and T. Takehisa. *Adv. Mater.*, 2002, **14**, 1120-1124.
32 Y. Liu, M. Zhu, X. Liu, W. Zhang, B. Sun, Y. Chen and H. J. P. Adler, *Polymer*, 2006, 47, 1–5.
33 X. Tong, J. Zheng, Y. Lu, Z. Zhang and H. Cheng, *Mater. Lett*., 2007, **61**, 1704-1706.
34 R. Dash, M. Foston and A. J. Ragauskas, *Carbohydr. Polym.*, 2013, **91**, 638-645.
35 M. A. Rafiee, J. Rafiee, Z. Wang, H. H. Song, Z. Z. Yu and N. Koratkar, *ACS Nano*, 2009, **3**(12), 3884-3390.
36 Z. X. Tai, J. Yang, Y. Y. Qi, X. B. Yan and Q. J. Xue. *RSC Adv.*, 2013, **3**, 12751-12757.
37 J. Liang, Y. Xu, Y. Huang, L. Zhang, Y. Wang, Y. F. Ma, F. F. Li, T. Y. Guo and Y. S. Chen, *J. Phys. Chem. C*, 2009, **113**(22), 9921-9927.
38 C. C. Teng, C. C. Ma, C. H. Lu, S. Y. Yang, S. H. Lee, M. C. Hsiao, M. Y. Yen, K. C. Chiou and T. M. Lee, *Carbon*, 2011, **49**(15), 5107-5116.
39 J. C. Fan, Z. X. Shi, M. Lian, H. Li and J. Yin, *J. Mater. Chem. A*, 2013, **1**, 7433-7443.
40 K. Chu, W. S. Li and F. L. Tang, *Phys. Lett. A*, 2013, **377**(12), 910-914.

Journal Name

Dynamic Article Links ►

Cite this: DOI: 10.1039/c0xx00000x

www.rsc.org/xxxxxx

ARTICLE TYPE

41 R. Q. Liu, S. M. Liang, X. Z. Tang, D. Yan, X. F. Li and Z. Z. Yu, *J. Mater. Chem.*, 2012, **22**, 14160-14167.
42 H. P.Cong, P. Wang and S. H. Yu, *Chem. Mater.*, 2013, **25**, 3357-3362.
43 Y. Bao, J. Z. Ma and Y. G. Sun, *Carbohydr. Polym*., 2012, **88**, 589-595.
44 R. T. Cha, Z. B. He and Y. H. Ni, *Carbohydr. Polym.*, 2012, **88**, 713-718.
45 M. D. Torres, R. Moreira, F. Chenlo and Vazquez MJ, *Carbohydr Polym.,* 2012, **89**, 592-598.
46 J. H.Ma, Y. J. Xu, B. Fan and B. R. Liang, *Europ. Polym. J*., 2007, **43**, 2221-2228.
47 W. B. Wang and A. Q. Wang*, Carbohydr. Polym*., 2010, **82**, 83-91.
48 W. B. Wang and A. Q. Wang, *Polym. Adv. Technol*., 2011, **22**, 1602-1611.
49 M. Yadava, K. Y. Rheea and S. J. Park, *Carbohydr. Polym,*. 2014, **110**, 18–25.
50 Devlin A. J., P. V. Hatton and Brook I. M. *J. Mater. Sci. Mater. Med.*, 1998, **9**(12): 737-741.
51 Y. X. Xu, K. X. Sheng, C. Li and G. Q. Shi*, ACS Nano*, 2010, **4**, 4324-4330.
52 Y. G. Seol, T. Q. Trung, O. J. Yoon, I. Y. Sohn and N. E. Lee, *J. Mater. Chem*., 2012, **22**, 23759-23766.
53 L. Guo, H. Sato, T. Hashimoto and Y. Ozaki, *Macromolecules*, 2010, **43**, 3897-3902.
54 M. M. Coleman, D. J. Skrovanek, J. Hu and P. C. Painter, *Macromolecules*, 1988, **21**, 59-65.
55 J. H. Liu, G. S. Chen and M. Jiang, *Macromolecules*, 2011, **44**, 7682-7691.
56 Y. Q. Chen, L. B. Chen, H. Bai, and L. Li, *J. Mater. Chem. A,* 2013, **1**, 1992-2001
57 Y. W. Huang, M. Zeng, J. Ren, J. Wang, L. R. Fan and Q. Y. Xu, *Colloids. Surf. A,* 2012, **401**, 97-106.
58 J. F. Shen, B. Yan, T. Li, Y. Long, N. Li and M. X. Ye. *Soft Matter,* 2012, **8**, 1831-1836.
59 N.M. Franson and N.A. Peppas *, J. Appl. Polym. Sci.*, 1983, **28**(4), 1299-1310.
60 C. C. R. Robert, P. A. Buri and N. A. Peppas, *J. Appl. Polym. Sci.,* 1985, **30**(1), 301-306.
61 I. J. Suarez, B. Sierra-Martin and A. Fernandez-Barbero, *Colloids Surf. A: Physicochem. Eng. Aspects*, 2009, **343**, 30-33.
62 J. Sjostrom and L. Piculell, *Colloids Surf. A: Physicochem. Eng. Aspects,* 2001, **183-185**, 429-448.
63 H. J. Schott, *Macromol. Sci. Phys.*, 1992, **31**, 1-9.
64 S. Xu, L. Fan, M. Zeng, J. Wang and Q. Liu, *Colloid. Surf. A Physicochem. Eng. ,* 2010, **371**, 59-63.